Supplementary Figure 1

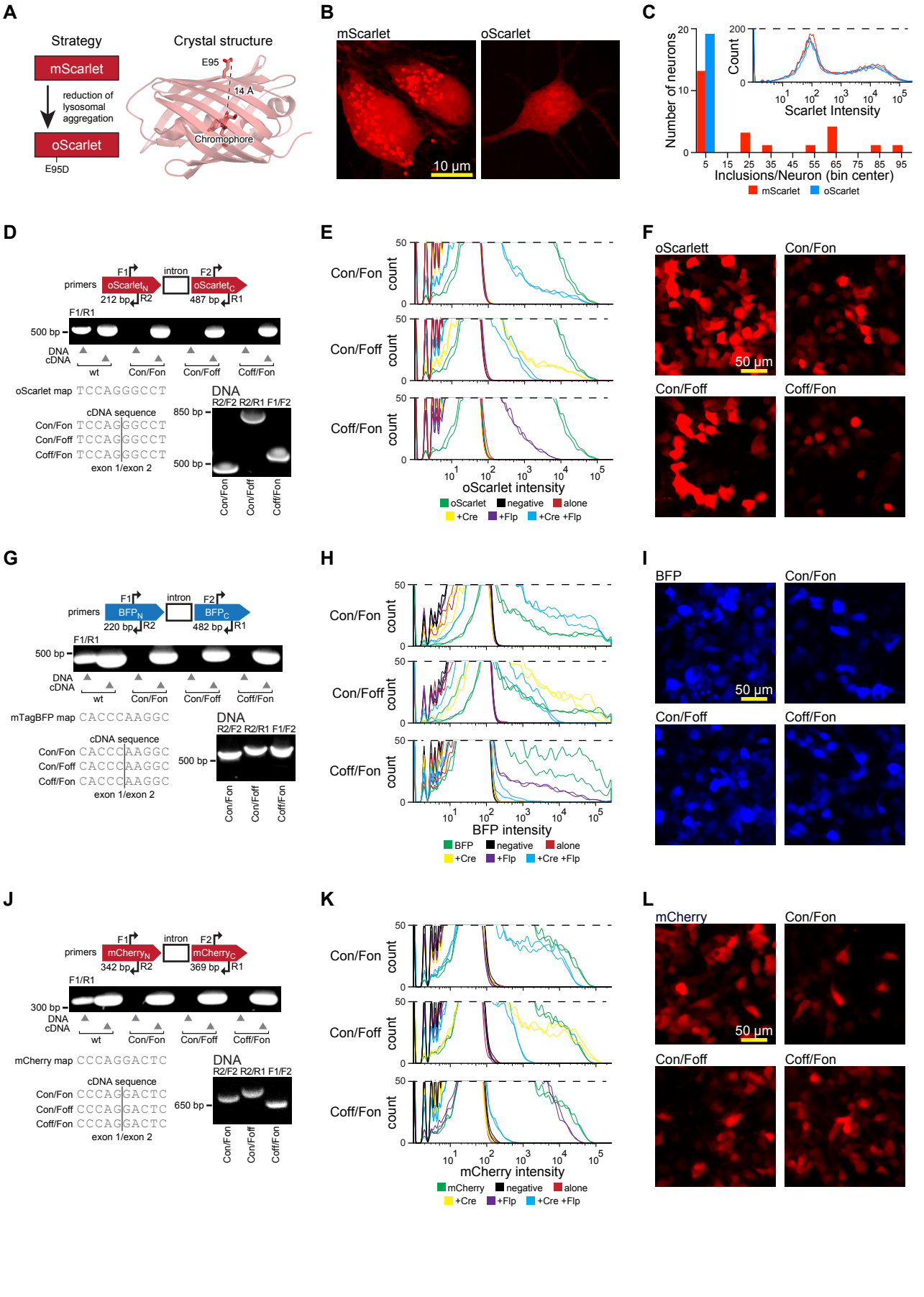

Supplemental Figure 1. INTRSECT fluorophore development, related to Figures 1 and 2. A-C) Optimization of mScarlet. A) We hypothesized that disrupting a lysosomal targeting motif by introducing mutation E95D would reduce aggregation without impairing fluorophore function. B) Cultured neurons expressing mScarlet show obvious aggregates while the mScarlet(E95D) mutant ('oScarlet') do not. C) Summary histogram of aggregates in neurons transfected with mScarlet (red, n=24) or oScarlet (blue, n=19) showing reduced aggregation of oScarlet (mean aggregates oScarlet = 0.579 per neuron, mScarlet = 25.92 per neuron, $p < 0.0001$, Mann-Whitney), while flow cytometry profiling of HEK293 cells transfected with these constructs show equivalent expression (*inset*). Development of INTRSECT oScarlet (D-F), INTRSECT mTagBFP (G-I), and INTRSECT mCherry (J-L). D,G,J) PCR of INTRSECT plasmid DNA does not generate an amplicon while PCR of cDNA from cells co-transfected with same plasmids and activating recombinases results in single expected band (*middle*); the sequences of these cDNA bands are seamless across the exon junction (*bottom-left*). PCR of INTRSECT plasmid DNA generated expected bands with orientation-specific primers (*bottom-right*). E,H,K) Flow cytometry of cells transfected with INTRSECT constructs and indicated recombinases shows high expression for Con/Fon and Con/Foff, while Coff/Fon is modestly lower than WT. Con/Foff shows diminished, but residual, expression when co-transfected with Cre and Flp, while Coff/Fon expression is either indistinguishable from negative control (E) or has a minor, dim residual population (H,K) when co-transfected with Cre and Flp. F,I,L) INTRSECT fluorophores are highly expressed in HEK293 cells when co-transfected with activating recombinases.

Supplementary Figure 2

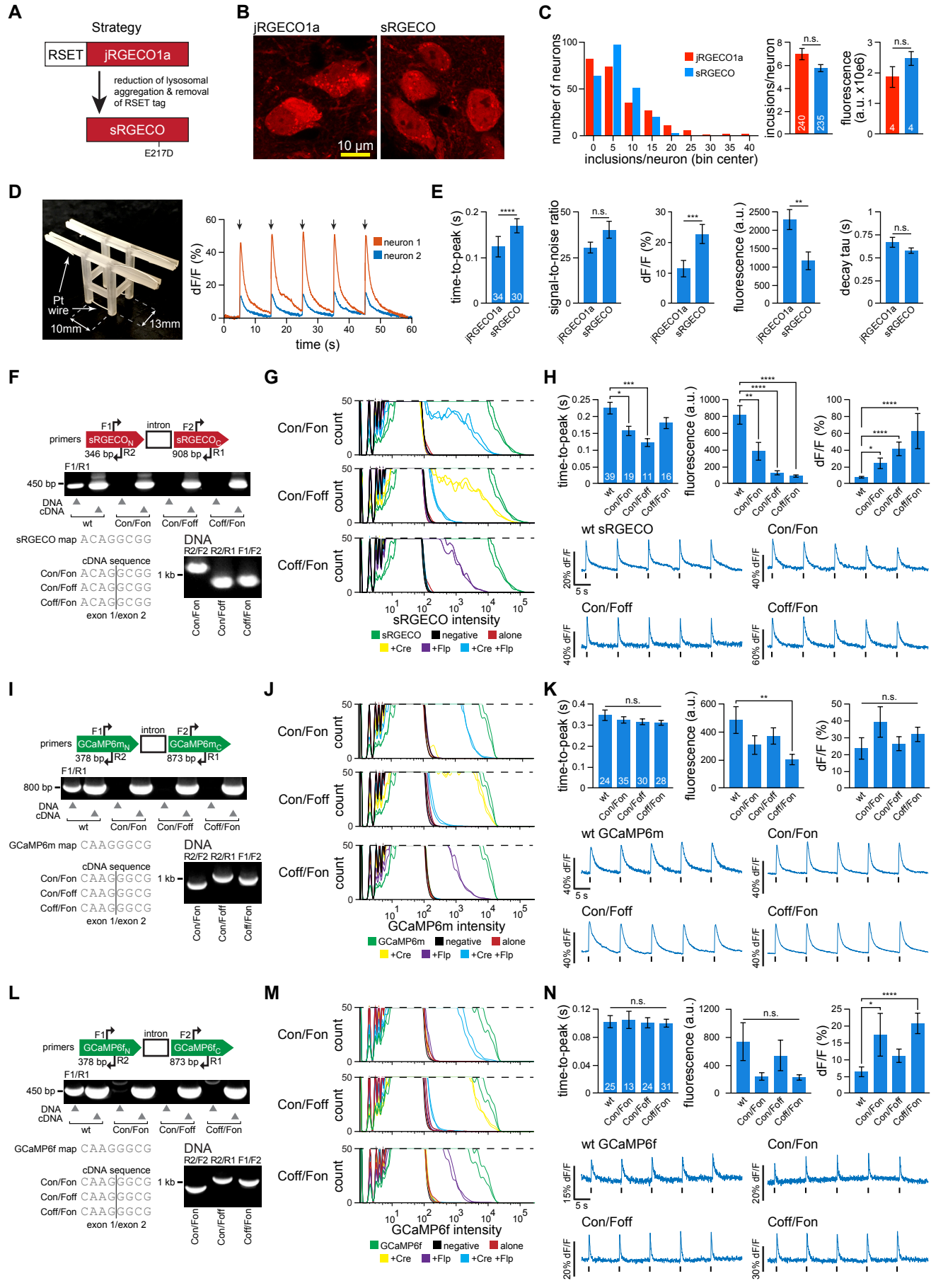

Supplemental Figure 2. INTRSECT GECI development, related to Figures 1 and 2. A-E) Optimization of jRGECO1a. A) To reduce payload size and decrease observed *in vivo* aggregation, we removed the RSET sequence and disrupted a putative lysosomal targeting motif by introducing mutation E217D to create sRGECO. B) Representative neurons from mouse mPFC four weeks after infection with either jRGECO1a (*left*) or sRGECO (*right*). C) Summary histogram of aggregates per neuron after four weeks of expression *in vivo* (*left*). The distribution of aggregates in sRGECO were significantly less than jRGECO1a (*left;* $p = 0.0368$, Kolmogorov-Smirnov test), while average number of aggregates per neuron in sRGECO (*middle*; 5.732, $n = 235$) was not significantly less than jRGECO1a (6.958, $n = 240$; $p = 0.7846$, Mann-Whitney test). Fluorescence expression did not differ between constructs *in vivo* (*right;* $n = 4$ injection sites each, mean total integrated fluorescence sRGECO = 2.47 x 10e7 A.U., jRGECO1a = 1.86 x 10e7 A.U., $p = 0.1867$, unpaired t-test). D) To characterize sRGECO function, we constructed a 3D-printed well insert for field stimulation (*left*) that reliably drove signal in cultured neurons expressing Con/Fon-GCaMP6m (*right*). E) sRGECO and jRGECO1a had broadly similar biophysical properties in cultured neurons, albeit with lower basal fluorescence of sRGECO with associated increase in dF/F ($p < 0.01$, unpaired t-tests, n as indicated). Development of INTRSECT sRGECO (F-H), INTRSECT GCaMP6m (I-K), and INTRSECT GCaMP6f (L-N). F,I,L) PCR of INTRSECT plasmid DNA does not generate an amplicon while PCR of cDNA from cells co-transfected with same plasmids and activating recombinases results in single expected band (*middle*); the sequences of these cDNA bands are seamless across the exon junction (*bottom-left*). PCR of sRGECO plasmid DNA generated expected bands with orientation-specific primers (*bottom-right*). G,J,M) Flow cytometry of cells transfected with INTRSECT tools and indicated recombinases show generally high expression comparable to WT, with diminished lower expression in the active configuration of Con/Fon and Coff/Fon. A minor population of cells co-transfected with Cre and Flp are not fully inactivated. H,K,N) INTRSECT tools co-transfected in cultured neurons generate reliable calcium signal in response to field stimulation, with some scattered differences in biophysical properties (*top*; n as indicated, * $p < 0.05$, ** $p < 0.01$, *** $p < 0.005$, **** $p < 0.0005$, Kruskal-Wallis test with Dunn's test). Exemplar %dF/F traces from culture neuron stimulation show reliable signal from all INTRSECT configurations (*bottom*).

Supplementary Figure 3

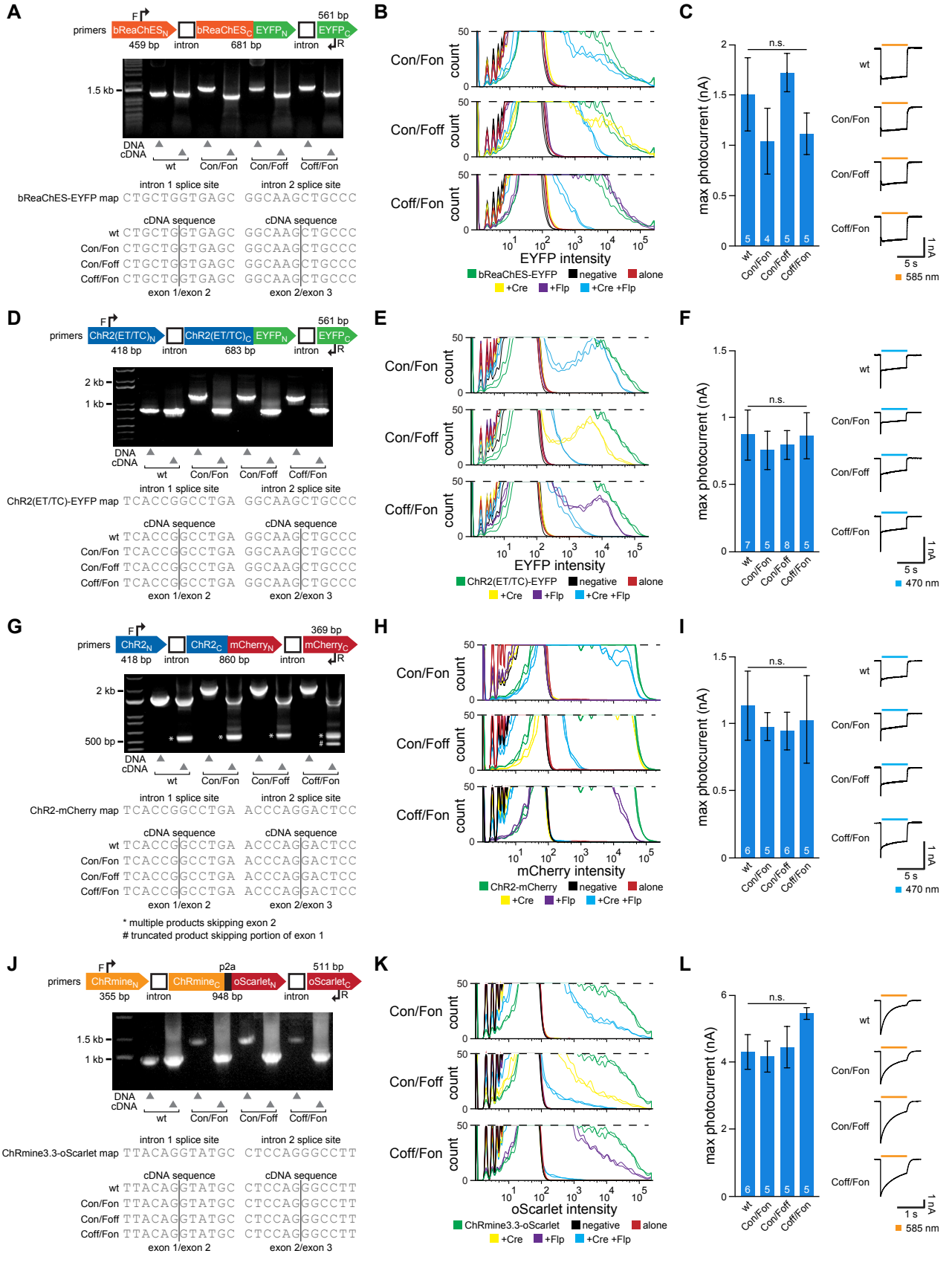

Supplemental Figure 3. INTRSECT excitatory opsin development, related to Figures 1 and 2. Development of INTRSECT bReaChES-EYFP (A-C), INTRSECT ChR2(ET/TC)-EYFP (D-F), INTRSECT ChR2(H134R)-mCherry (G-I), and INTRSECT ChRmine3.3-p2a-oScarlet (J-L). A,D,G,J) PCR of INTRSECT plasmid DNA generates an amplicon larger than WT, while PCR of cDNA from cells co-transfected with same plasmids and activating recombinases results in an amplicon equivalent to WT (*middle*). The sequences of these cDNA bands are seamless across the exon junctions (*bottom*). INTRSECT ChR2(H134R)-mCherry was additionally noted to have a smaller PCR product generated by all four cDNA templates and a second, unique product for Coff/Fon. The shared minor amplicon is a truncated sequence splicing exon 1 to exon 3 directly, including in the non-intron-containing WT (noted by *). The tertiary product of Coff/Fon represents a cryptic splice site active only in this logical configuration (*bottom*, noted by #). B,E,H,K) Flow cytometry of cells transfected with INTRSECT tools and indicated recombinases show expression comparable to WT. Diminished, but residual, expression is observed in all constructs for the Con/Foff configuration and in various constructs (B,E) for the Coff/Fon configuration when co-transfected with Cre and Flp. C,F,I,L) Photocurrents of INTRSECT excitatory opsins co-transfected with activating recombinases in cultured neurons are equivalent to WT (*left*; all vs. WT, bReaChES-EYFP $p > 0.5$ for all comparisons, ChR2(ET/TC)-EYFP $p > 0.9$ for all comparisons, ChR2(H134R)-mCherry $p > 0.85$ for all comparisons, ChRmine3.3-p2a-oScarlett $p > 0.2$ for all comparisons, n as indicated, ANOVA with Dunnett's test). Exemplar recordings from whole-cell electrophysiology recordings show reliable excitatory photocurrent from all INTRSECT configurations (*right*).

Supplementary Figure 4

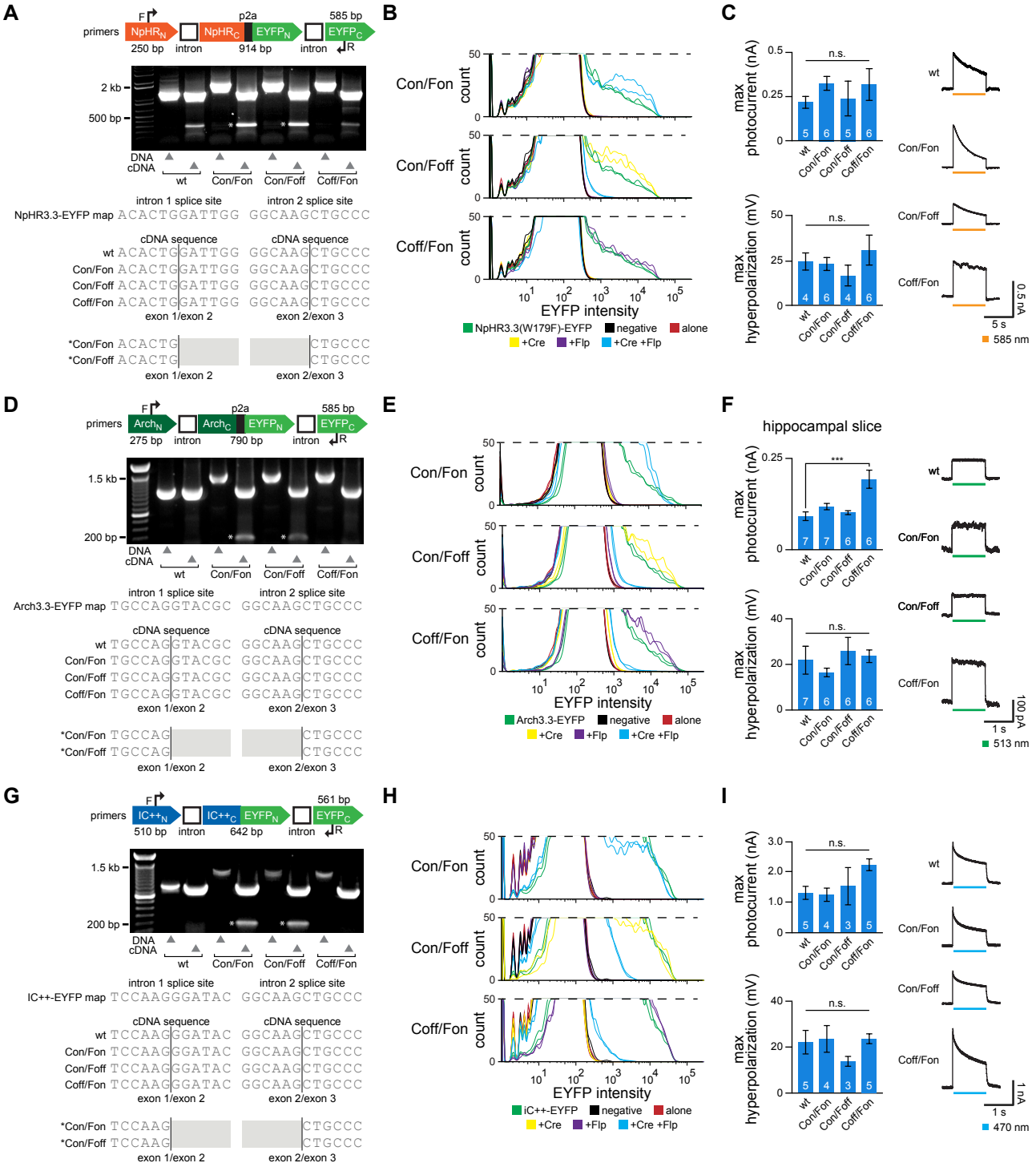

Supplemental Figure 4. INTRSECT inhibitory opsin development, related to Figures 1 and 2. Development of INTRSECT NpHR3.3-p2a-EYFP (A-C), INTRSECT Arch3.3-p2a-EYFP (D-F), and INTRSECT iC++-EYFP (G-I). A,D,G) PCR of INTRSECT plasmid DNA generates an amplicon larger than WT, while PCR of cDNA from cells co-transfected with same plasmids and activating recombinases results in an amplicon equivalent to WT (*middle*); a smaller PCR product is noted in all tools for Con/Fon and Con/Foff. The sequences of these cDNA bands are seamless across the exon junctions. The shared minor amplicon (noted by *) is a truncated sequence splicing exon 1 to exon 3 directly; high-quality sequencing of minor products for NpHR3.3-p2a-EYFP (A) was only obtained for Con/Fon and Con/Foff PCR products. B,E,H) Flow cytometry of cells transfected with INTRSECT tools and indicated recombinases show expression comparable to WT. Diminished, but residual, expression is observed in all constructs for the Con/Foff configuration and in some constructs (E,H) for the Coff/Fon configuration when co-transfected with Cre and Flp. C,F,I) Maximum photocurrents and hyperpolarizations of INTRSECT tools co-transfected with activating recombinases in cultured neurons are equivalent to WT for NpHR3.3-p2a-EYFP and iC++-EYFP (*left*; all vs. WT, NpHR3.3-p2a-EYFP $p > 0.9$ for all comparisons, iC++-EYFP $p > 0.05$ for all comparisons, n as indicated, ANOVA with Dunnett's test, measurements of the chloride channel iC++ taken at -40mV (Berndt et al., 2016)). INTRSECT Arch3.3-p2a-EYFP showed reduced photocurrents for Con/Fon and Con/Foff (all vs. WT, Con/Fon $p = 0.0143$, Con/Foff $p = 0.0123$, Coff/Fon $p = 0.4551$, n as indicated, ANOVA with Dunnett's test) and reduced hyperpolarization for Con/Foff (all vs. WT, Con/Fon $p = 0.2730$, Con/Foff $p = 0.0264$, Coff/Fon $p = 0.1252$, n as indicated, ANOVA with Dunnett's test). Acute mPFC slice recordings from neurons expressing WT and INTRSECT Arch3.3-p2a-EYFP four weeks post-infection showed equivalent photocurrents for these two logical configurations and significantly increased photocurrent for Coff/Fon (F-*top left*; all vs. WT, n as indicated, Con/Fon $p = 0.3966$, Con/Foff $p = 0.9286$, Coff/Fon $p = 0.0001$, ANOVA with Dunnett's test), while hyperpolarization in slice are equivalent to WT (F-*bottom left;* all vs. WT, $p > 0.75$ for all comparisons, n as indicated, ANOVA with Dunnett's test). Exemplar recordings from whole-cell electrophysiology recordings show reliable inhibitory photocurrent from all INTRSECT configurations (C,F,I - *right*).

Supplementary Figure 5

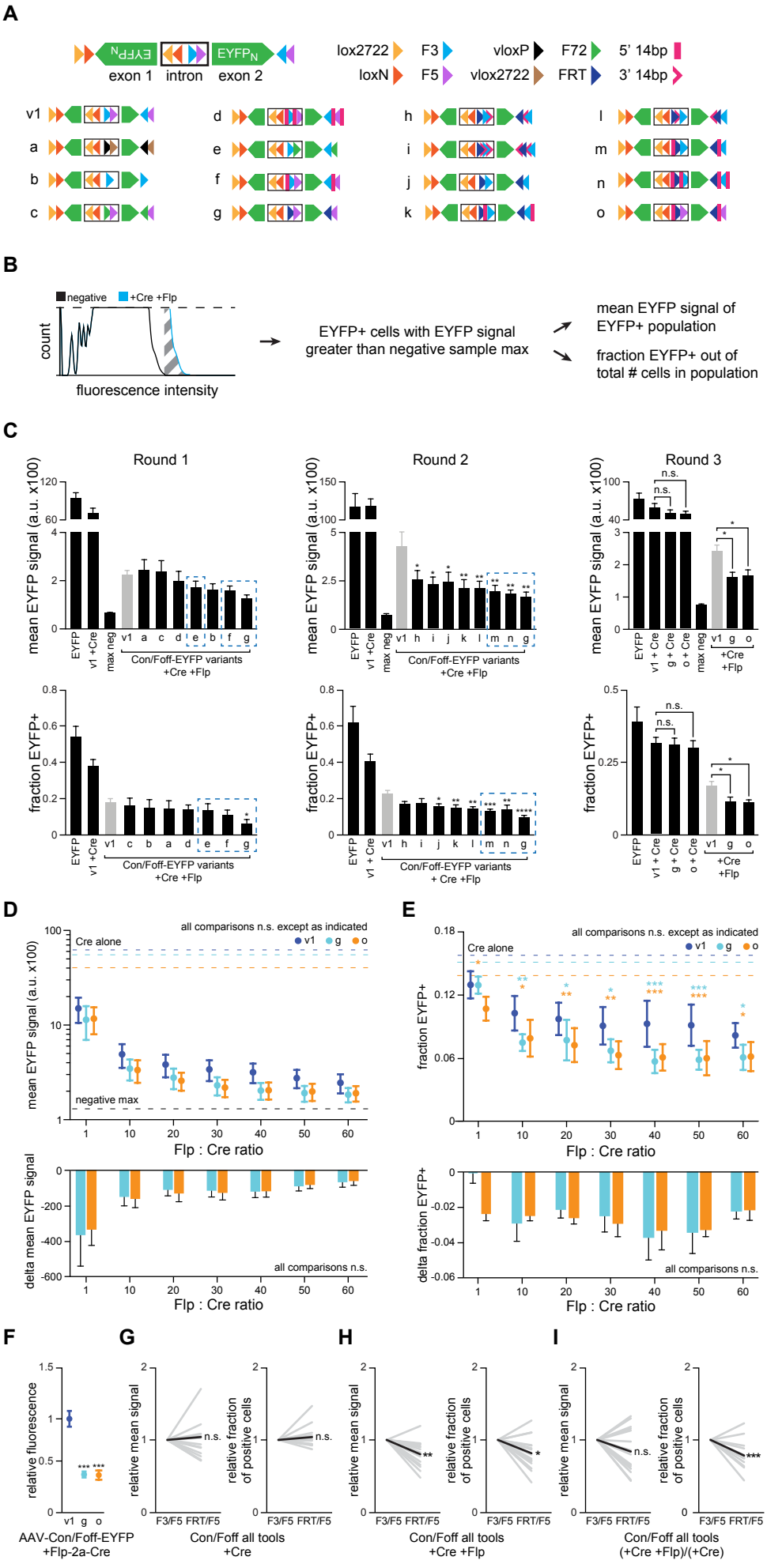

Supplemental Figure 5. Optimization of the Con/Foff INTRSECT backbone, related to Figure 3. A) Con/Foff-EYFP variants with modified sequences noted by triangles (recombinase recognition sequences) and bars (additional 14bp sequences). Triangle direction notes orientation of central recognition site motif relative to promoter. The original INTRSECT 'F3/F5' cassette is noted throughout by 'v1'. B) Variants were screened by flow cytometry and the residual population was defined as having fluorescence intensity greater than the maximum intensity of the negative control. Mean EYFP signal of this residual population and percentage of total population remaining positive, were used as the read-outs of variant function. C) Variants were refined sequentially through three rounds of screening. FRT/F5 ('g') and 14bp-FRT/F5 ('o') were consistently superior to v1 with significantly decreased mean signal and percentage of total population (n = 5 separate experiments, all vs. v1, * $p < 0.05$, ** $p < 0.01$, *** $p < 0.001$, **** $p < 0.0005$; ANOVA with Dunnett's test). Dashed blue boxes indicate variants further modified in subsequent screening round. There was no difference in high expression levels of variants 'g' or 'o' in the active configuration. D,E) Two Con/Foff-EYFP variants ('g', 'o') decrease residual expression mean EYFP fluorescence (D) and the fraction of residual cells (E) compared to Con/Foff(F3/F5)-EYFP ('v1') over a broad range of Flp:Cre ratios in co-transfected HEK293 cells (compared to v1, * $p < 0.05$, ** $p < 0.01$, *** $p < 0.001$, **** $p < 0.0001$, n = 5 independent experiments, ANOVA with Dunnett's test), although further increasing the ratio beyond 10:1 showed marginal further increase toward the fitted plateau values (R^2 mean expression v1 = 0.8028, g = 0.7114, o = 0.6921; R^2 fraction of residual cells v1 = 0.2793 g = 0.5848, o = 0.3983). There was no significant difference in the magnitude of improvement for either residual fluorescence (D-*bottom*) or fraction of residual EYFP+ cells (E-*bottom*) between the two improved variants ($p > 0.25$ for all comparisons, ANOVA with Sidak's test). F) Decreased residual expression was maintained *in vivo* for both variants 'g' and 'o' relative to 'v1' in animals co-injected with viral Con/Foff variants and Cre-2a-Flp (data normalized to AAV-Cre controls, residual fluorescence relative to v1: g = 0.4066, p = 0.0009, n = 3 animals, o = 0.4003, p = 0.0008, n = 3 animals, ANOVA with Dunnett's test). The FRT/F5 variant ('g') was chosen for the Con/Foff INTRSECT backbone to facilitate cloning. G-I) Comparison of mean signal (*left*) and percentage of total population (*right*) of all 15 INTRSECT Con/Foff tools in the FRT/F5 configuration relative to original (F3/F5) versions in HEK293 cells co-transfected with Cre alone (G; active configuration; mean relative signal of FRT/F5 = 1.046, p = 0.4578, relative percentage of total population = 1.038, p = 0.4733), co-transfected with Cre AND Flp (H; inactivated configuration, relative mean signal = 0.807, p = 0.0069, relative percentage of total population = 0.8214, p = 0.0101, n = 15 individual constructs, all comparisons paired t-tests). I) Data from (*H*) normalized to Cre alone controls (normalized relative mean signal = 0.8445, p = 0.0795, normalized relative percentage of total population = 0.7894, p = 0.0010, paired t-tests).

Supplementary Figure 6

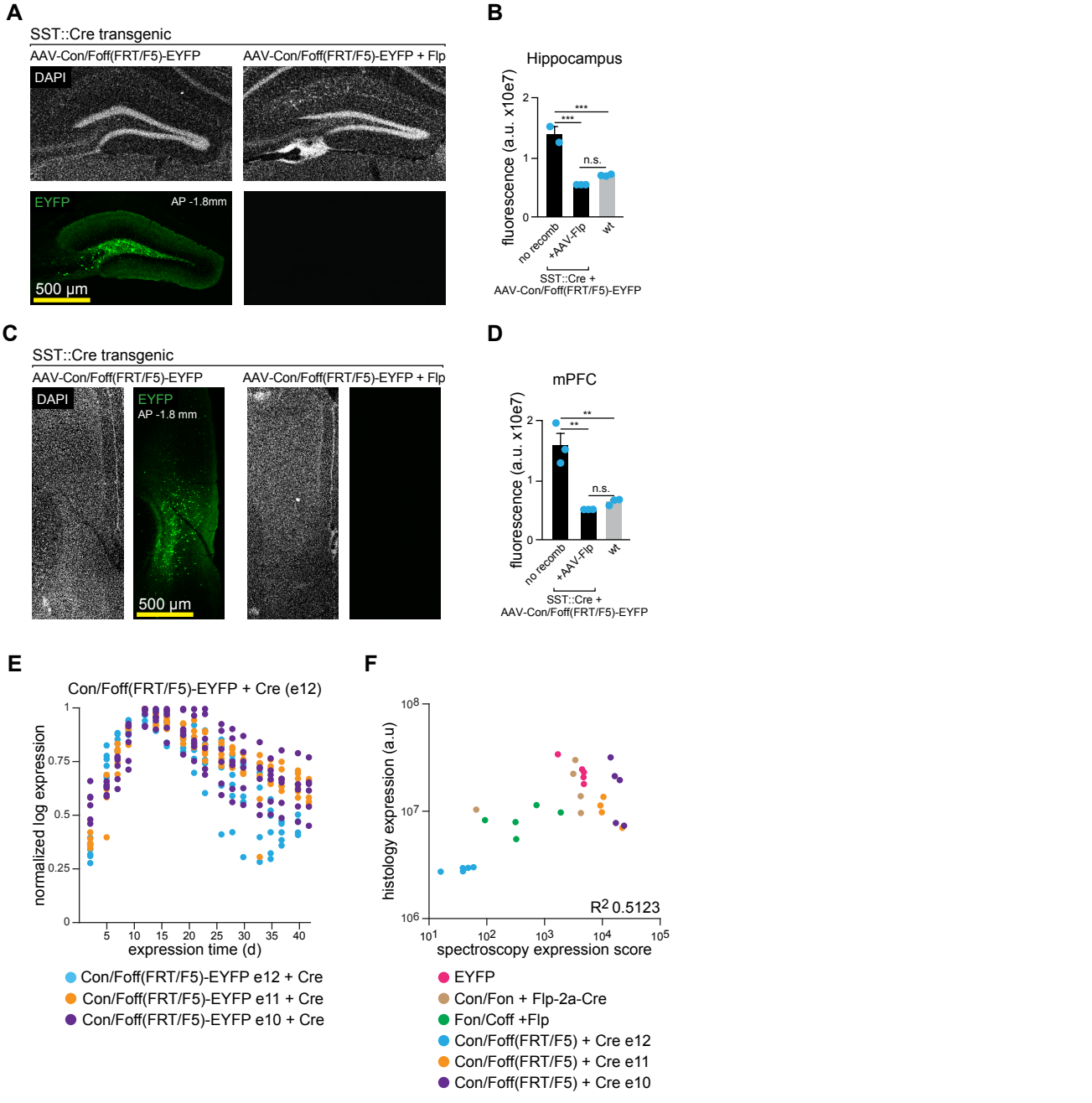

Supplemental Figure 6. Con/Foff(FRT/F5) is highly efficient *in vivo*, related to Figure 3. A-D) AAV-Con/Foff(FRT/F5)-EYFP is highly expressed in a Cre transgenic mouse and is inactivated by AAV-Flp. A,C) Injection of AAV-Con/Foff(FRT/F5)-EYFP in the hippocampus (A) or mPFC (C) of a SST-Cre transgenic mouse shows expected high expression when injected alone (*left*) which is inactivated when co-injected with AAV-Flp (*right*). DAPI for comparison. B,D) SST-Cre animals show a consistently high level of expression when injected with AAV-Con/Foff(FRT/F5)-EYFP alone in the hippocampus (B; vs. AAV-Flp $p = 0.0003$; vs WT $p = 0.0007$; ANOVA with Tukey's test) or mPFC (D; vs. AAV-Flp $p = 0.0014$; vs WT $p = 0.0027$, ANOVA with Tukey's test), while expression in animals co-injected with AAV-Flp is indistinguishable from wild-type animals (hippocampus $p = 0.1481$, mPFC $p = 0.7208$, ANOVA with Tukey's test). E) Observed *in vivo* viral toxicity observed with high titers of AAV-Cre (Figure 3H) is independent of AAV-Con/Foff(FRT/F5)-EYFP titer. F) Comparison of the measured *in vivo* viral expression score immediately prior to animal sacrifice and post-hoc total integrated fluorescence measured by confocal are positively correlated ($R^2 = 0.5123$, $p < 0.0001$, $n = 30$, Pearson correlation of log-transformed data).

Supplementary Table 1

Oligo Name	Sequence (5’ -> 3’)
Sequencing nEF F	GACCCTGCTTGCTCAACTCT
Sequencing EF1a F	TGGAATTTGCCCTTTTTGAG
Sequencing Intron 1 F	GGGACGACATGACTTAACCAG
Sequencing Intron 1 R	CCAGCCCTTCTCATGTTCAG
Sequencing Intron 2 F (only 2-intron constructs)	CCTGTATGTGACCCATGTGC
Sequencing Intron 2 R (only 2-intron constructs)	GCACATGGGTCACATACAGG
Sequencing WPRE R	GGGCCACAACTCCTCATAAA
Arch-EYFP RT F	CTTCTACTTTCTGGTCCGCG
Arch-EYFP RT R	AAGTCGTGCTGCTTCATGTG
BFP RT F	ACCGTGGACAACCATCACTT
BFP RT R	ATGTCGTTTCTGCCTTCCAG
bREACHes-EYFP RT F	GACCAGCTACACCCTGGAGA
bREACHes-EYFP RT R	AAGTCGTGCTGCTTCATGTG
ChR2-EYFP RT F	CAATGTTACTGTGCCGGATG
ChR2-EYFP RT R	AAGTCGTGCTGCTTCATGTG
ChR2-mCherry RT F	CAATGTTACTGTGCCGGATG
ChR2-mCherry RT R	CTTGTACAGCTCGTCCATGC
GCaMP6M RT F	ACTTCAAGATCCGCCACAAC
GCaMP6M RT R	TCCCCGTCCTTGTCAAATAG
GCaMP6F RT F	ACTTCAAGATCCGCCACAAC
GCaMP6F RT R	TCCCCGTCCTTGTCAAATAG
iC++-EYFP RT F	AACAAGCGTACCATGGGTCT
iC++-EYFP RT R	AAGTCGTGCTGCTTCATGTG
mCherry RT F	CCTGTCCCCTCAGTTCATGT
mCherry RT R	CTTCAGCTTCAGCCTCTGCT
NpHR-EYFP RT F	GTTGTTCGAGTTCGTGCTGA
NpHR-EYFP RT R	AAGTCGTGCTGCTTCATGTG
oScarlet RT F	CCATGAACGGCCACGAGTTCG
oScarlet RT R	GTCCAACTTGCGGTCCACGTTG
srGECO RT F	CAACGAGGACTACACCATCG
srGECO RT R	GTCCTCGAAGTTCATCACGC
3xEYFP RT F	AGCTGGACGGCGACGTAAA
3xEYFP RT R	GCTCGTCCATGCCGAGAGTG
3xGCaMP6M RT F	GATCACATGGTCCTGCTGGA
3xGCaMP6M RT R	ATCCCCATCGATGTCTGCTT

Supplementary Table 1. cDNA sequencing and reverse transcription DNA oligos, related to Figures 2,5,s1-s4. DNA oligos used for routine plasmid sequencing and quality control (Oligo Names staring with 'Sequencing') and oligos used for RT-PCR and PCR product sequencing (Oligo Names containing 'RT'). 'F' denotes forward (sense) primer, 'R' denotes reverse (anti-sense) primer. 'Sequencing' primers designed to bind to promoter sequence ('nEF' and 'EF1a'), within the conserved intron regions ('intron X'), or WPRE element. RT-PCR primers sit within ORF of noted plasmids; for two-intron constructs (e.g. ChR2-EYFP), F primer binds within exon 1 while R primer binds within exon 3, with both splice sites in between. Sequences given 5' to 3'. All oligos synthesized by IDT.